

AUGUST 09 2023

Basin scale coherence of Kauai-Beacon *m*-sequence transmissions received at Wake Island and Monterey, CA

FREE

Kay L. Gamba ; Nicholas C. Durofchalk ; David R. Dall'Osto; Rex K. Andrew; Paul Leary; Bruce M. Howe ; Kevin B. Smith



JASA Express Lett 3, 080801 (2023)

<https://doi.org/10.1121/10.0020514>



View
Online



Export
Citation

CrossMark

Related Content

Basin-scale propagation modeling of MLS signals between Kauai and Monterey

J Acoust Soc Am (October 2022)

Applications of an ultra low-drag towed array deployed from a glider

J Acoust Soc Am (May 2007)

Using Seagliders for acoustic receiving and communication


J Acoust Soc Am (May 2008)



Advance your science and career as a member of the
Acoustical Society of America

[LEARN MORE](#)

Basin scale coherence of Kauai-Beacon m -sequence transmissions received at Wake Island and Monterey, CA

Kay L. Gemba,^{1,a)}  Nicholas C. Durofchalk,¹  David R. Dall'Osto,² Rex K. Andrew,² Paul Leary,¹ Bruce M. Howe,³  and Kevin B. Smith¹

¹Department of Physics, Naval Postgraduate School, Monterey, California 93943, USA

²Applied Physics Laboratory, University of Washington, Seattle, Washington 98105, USA

³School of Ocean and Earth Science and Technology, University of Hawaii at Manoa, Honolulu, Hawaii 96822, USA

kay.gemba@nps.edu; nicholas.durofchalk@nps.edu; dallosto@uw.edu; aplur.rxandrew@gmail.com; pleary@nps.edu; bhowe@hawaii.edu; kbsmith@nps.edu

Abstract: The 75 Hz Kauai-Beacon source is well-situated for observing the North Pacific Ocean acoustically, and ongoing efforts enable transmissions and analysis of broadband signals in 2023 and beyond. This is the first demonstration of acoustic receiving along paths to Wake Island (~3500 km) and Monterey Bay (~4000 km). The 44 received m -sequence waveforms exhibit excellent phase stability with processing gain approaching the maximum theoretical gain evaluated over the 20 min signal transmission duration. The article concludes with a discussion on the future source utility and highlights research topics of interest, including observed Doppler (waveform dilation), thermometry, and tomography.

[Editor: David R. Barclay]

<https://doi.org/10.1121/10.0020514>

Received: 19 April 2023 Accepted: 20 July 2023 Published Online: 9 August 2023

1. Observing the ocean acoustically

The Kauai-Beacon (KB) source first transmitted its coded thermometry signal in 1997, and in operation from 1998–2006, measured the ocean and generated critical data to improve oceanographic models. After recent repairs to its infrastructure, the source, once again, is operational. Now, 15 yrs later and with distant and remote ocean observatories continuously monitoring the Pacific Ocean acoustically, the Beacon is transmitting its thermometry signal on a regular interval—for 20 min, 6 times a day, every 4th day, starting at the top of the UTC hour.

Located off of the north shore of the Hawaiian Island of Kauai, the KB source has nearly unobstructed underwater acoustic paths into the North and Northeast Pacific Ocean, with even a few paths into the Northwestern Pacific Ocean. The source is Global Positioning System (GPS) synchronized (with timing uncertainty order microseconds) and emits large time-bandwidth signals with source levels ranging from 185 to 190 dB re 1 μ Pa at 1 m (26–81 W, 56–94 Hz). These levels are comparable to the source levels of blue whales (*Balaenoptera musculus*), ranging¹ from 184.9 to 199.8 dB re 1 μ Pa at 1 m (25–777 W), and actually are lower than source levels of some container ships, which can reach 209 dB re 1 μ Pa at 1 m (6461 W, 10–100 Hz).² The values in units of watts are calculated with a constant density of 1030 kg/m³ and a sound speed of 1500 m/s. The KB waveform bandwidth (37.5 Hz) and period duration (27.28 s) can be used by receivers implementing matched-filter pulse-compression³ to yield 30.1 dB of coherent gain. As a result of this additional gain, the signal can be detected at ranges well in excess of 4000 km. A system with this range and timing accuracy⁴ provides a critical research resource in the North Pacific Ocean to develop and verify ocean climate state models⁵ and enables research and development for ranging remote underwater sensors.⁶

In the following, we examine a set of four test transmissions (Tx) from the KB source to receivers H11S2 (International Monitoring System) near Wake Island and MARS (Monterey Accelerated Research System) off of the coast of California in Monterey Bay. We report on the coherence time at both locations, which is observed to be much greater than a single waveform period, and the ability to extract Doppler (waveform dilation) from the received data. In addition to demonstrating the receptions and high quality of data received at these two remote and distant stations, this letter serves as a timely announcement that active transmissions are occurring and ongoing.

2. Signal transmission and receptions

The first tests of the KB in the 1990s confirmed the effectiveness of pulse-compression at basin scale ranges in the North Pacific Ocean,⁷ capitalizing on the long history of signal modulation techniques in underwater acoustic research.⁸

^{a)} Author to whom correspondence should be addressed.

Table 1. Octal 3471 *m*-sequence waveform parameters, phase-modulated at $\varphi_L = \tan^{-1}(\sqrt{L})$ for optimum signal-to-noise ratio (SNR). The sequence initialization is 0000000001. See Ref. 9 for additional details on *m*-sequence waveform properties, design, and processing.

	Register law	Number of shift register stages	Sequence length	Phase angle	Carrier frequency	Period duration	Digit duration	Band width	Carrier cycles/digit
Symbol	—	<i>n</i>	<i>L</i>	φ	<i>f_c</i>	<i>T_p</i>	<i>T_d</i>	BW	Q
Unit	Octal	[·]	[·]	Deg	Hz	s	ms	Hz	[·]
Value	3471	10	1023	88.2	75	27.28	26.667	37.5	2

Now, the KB is transmitting the same signal at the same schedule for which it was designed in the thermometry studies of the 1990s and 2000s. This *m*-sequence waveform has a 75 Hz carrier frequency with parameters listed in Table 1.

Specifically, a ten-bit linear shift register is used to generate this signal, whereas its samples are generated according to an octal law (the KB uses 3471). This pseudorandom noise (PRN) code generates a sequence of 1023 digits, each containing $Q = 2$ carrier cycles, which modulates the waveform with a phase shift according to the sign (± 1) of the digit and phase angle, φ . Digits are short-duration segments of the same period as the shortest pulse that the transducer can efficiently radiate (i.e., inverse of the transducer’s bandwidth). The reciprocal of the digit duration establishes the 37.5 Hz bandwidth. The duration of a single signal period is 27.28 s.

The utility of the PRN-code as a modulation sequence is due to the properties of its periodic autocorrelation sequence. Pulse-compression of this 27.28 s single-period, spread-spectrum signal yields a 27 ms impulse (i.e., the approximate duration of its digit), and the normalized autocorrelation sequence takes on a value of $-1/L$ away from its peak. The waveform is transmitted consecutively 44 times and circular processing of 43 waveforms requires exact periodicity. For a 20 min duration signal, the 44th period is not transmitted entirely. The signals analyzed in this letter are test Tx, which are listed in Table 2.

The nascent transducer network in Fig. 1(a) includes the KB source and three hydrophones. The KB source is located off of the north shore of Kauai, HI, at latitude 22.34915° N and longitude 159.56992° W and mounted in a heavy steel tripod about 2 m from the bottom at 810 m deep. A convenient and nearby reference hydrophone used to observe transmissions is part of Station ALOHA,⁶ permanently installed north of the nearby island of Oahu, east of Kauai at latitude 22.7387° N and longitude 158.0062° W. The 4728 m deep ALOHA Cabled Observatory is located at a 162 km distance, downslope, relative to the KB source.

The westerly receiver is part of the Comprehensive Nuclear Test Ban Treaty (CTBT) International Monitoring System,¹⁰ a hydroacoustic network comprised of ~2 km baseline triad arrays of hydrophones. These stations are designed to maximize the detection and localization of low-frequency sounds in the ocean, and the hydrophones are suspended on riser cables from the seafloor, often from favorable geological features that provide a maximum “field of view” of the ocean basin. The Wake Island station includes two triad arrays with one triad located north and another located south of the island (stations H11N and H11S, respectively). Both triads monitor the Pacific Ocean, noting that the KB signal is received on all hydrophones at Wake Island. Here, we use hydrophone H11S2, part of the south triad, for processing. The south station H11S is situated on the 10 square-km plateau of a guyot, rising to within 1200 m of the sea surface, roughly 100 km south of the Wake Island Atoll, where the data is telemetered to the database. Hydrophone H11S2 is suspended on a ~450 m long riser cable to the sound channel axis to a nominal depth of 742 m at latitude 18.4908° N and longitude 166.7050° W.

The easternmost receiver is part of the MARS.¹¹ The Geospectrum GTI M20–105 vector sensor (GeoSpectrum Technologies Inc., Dartmouth, Nova Scotia, Canada) samples at 8 kHz and is moored close to the seafloor at 890 m deep at latitude 36.7125° N and longitude 122.1869° W. Results only use its pressure channel data.

Figure 1(b) visualizes the basin scale propagation through the deep sound channel to the receivers near Wake Island and Monterey. The coherent transmission loss is estimated with a ray tracing model, where bathymetric and oceanographic data are derived from the GEBCO 2021 grid¹² and the 2018 National Oceanic and Atmospheric Administration

Table 2. KB source 2021 test transmission (Tx) schedule with varying source level in units of dB re 1 μ Pa at 1 m. Table 1 summarizes transmitted waveform parameters. POSIX (Unix timestamp) is the number of seconds that have elapsed since January 1, 1970 (midnight UTC/GMT).

Tx (number)	Marktime (POSIX)	Time (UTC)	Source level (dB)	Duration (s)	No. of periods (<i>M</i>)
1	1 624 572 044	2021-06-24 22:00:44	185.4	1200	44
2	1 624 574 539	2021-06-24 22:42:19	185.4	1200	44
3	1 624 577 055	2021-06-24 23:24:15	187.0	1200	44
4	1 624 579 834	2021-06-25 00:10:34	187.0	1200	44

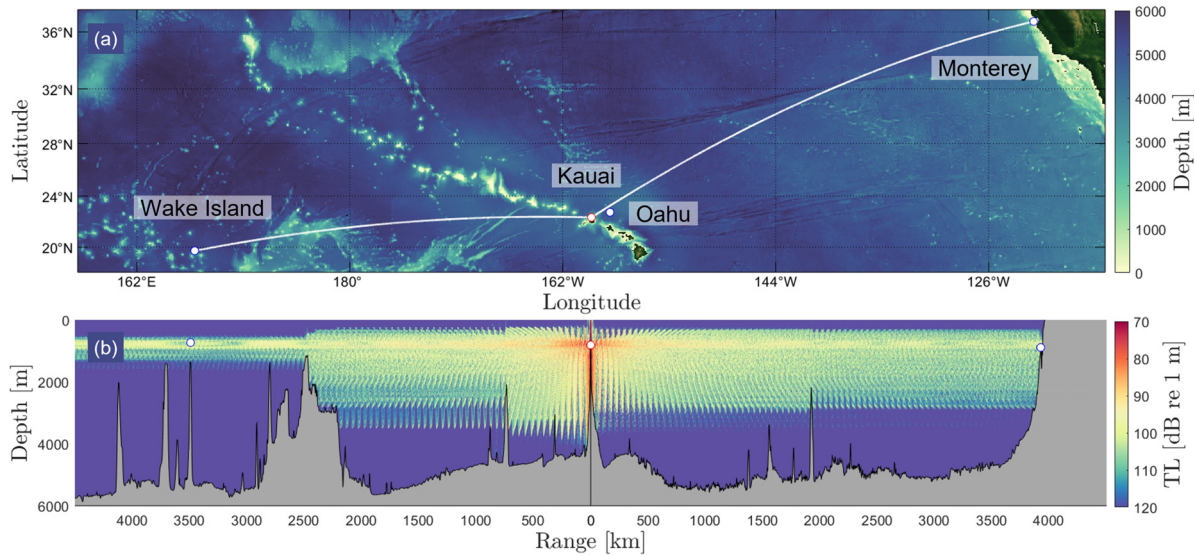


Fig. 1. (a) Nascent network of KB source and receiver locations. Station ALOHA located north of Oahu includes a convenient reference hydrophone used to observe source transmissions. (b) Ray tracing model shows propagation from the KB source (located north of Kauai) to receivers H11S2, Wake Island, and MARS, Monterey. The distance between the source and H11S2 (MARS) receiver is ~ 3500 (4000) km, corresponding to a travel-time of ~ 39 (44) min.

(NOAA) World Ocean Atlas annual averages, respectively. World Ocean Atlas sound speed estimates are derived from temperature and salinity data. Away from the source, the propagation is mostly non-bottom interacting with the exception of a few seamounts, which occasionally interrupt deep water refracting ray paths. The bathymetry and environmental conditions near the source¹³ are an important part of ongoing model development efforts to identify and associate early boundary interactions with the observed receiver arrival structure. The sediment is assumed to be medium silt or sand-silt-clay with sound speed of 1483 m/s, density of 1150 kg/m³, and attenuation factor of 0.37 dB per wavelength.¹⁴ Predicted transmission loss values for the two receivers using this preliminary model are included in Table 3.

3. Waveform processing at receivers H11S2 and MARS

The acoustic signal Tx numbers 1–4 listed in Table 2, which are part of a June 2021 validation test, are processed and analyzed. Results in Fig. 2 show a side-by-side comparison of the demodulated and matched-filtered receptions at each station for Tx number 4. Forty-three circularly processed *m*-sequence waveforms are averaged in Figs. 2(a) and 2(e) to increase processing gain (PG). Signal arrival time is estimated with eigenrays [Fig. 1(b)], which are assumed constant over the ~ 2 h Tx numbers 1–4 signal reception duration. Receptions are windowed for circularly processed waveforms (discarding approximately half of the first and last received periods) such that the channel impulse responses (CIRs) are centered

Table 3. Tx number 4 single receiver SNR = RL – NL + PG estimate for 43 circularly processed *m*-sequence periods at 3500 km (H11S2, Wake Island) and 4000 km (MARS, Monterey) range and 75 Hz center frequency in the Pacific Ocean. The nominal averaging gain across $M = 43$ periods is $8 \log_{10}(M)$ [see Figs. 2(d) and 2(h)].

	H11S2	MARS	
Source level [root mean square (rms)]	187.0	187.0	dB re 1 μ Pa at 1 m
Transmission loss	–107.5	–112.8	dB re 1 m
Attenuation (8.075×10^{-4} dB/km)	–2.9	–3.2	dB
Received level (RL)	76.6	71.0	dB re 1 μ Pa
Noise (1 Hz band, rms)	79.1	75.2	dB re 1 μ Pa ² /Hz
Mainlobe width (75 Hz)	18.8	18.8	dB re 1 Hz
Noise level (NL)	97.9	94.0	dB re 1 μ Pa
Pulse-compression gain (1023 digits)	30.1	30.1	dB
Averaging gain ($M = 43$ periods)	13.1	13.1	dB
Processing gain (PG)	43.2	43.2	dB
Receiver signal-to-noise ratio (SNR)	21.9	20.2	dB

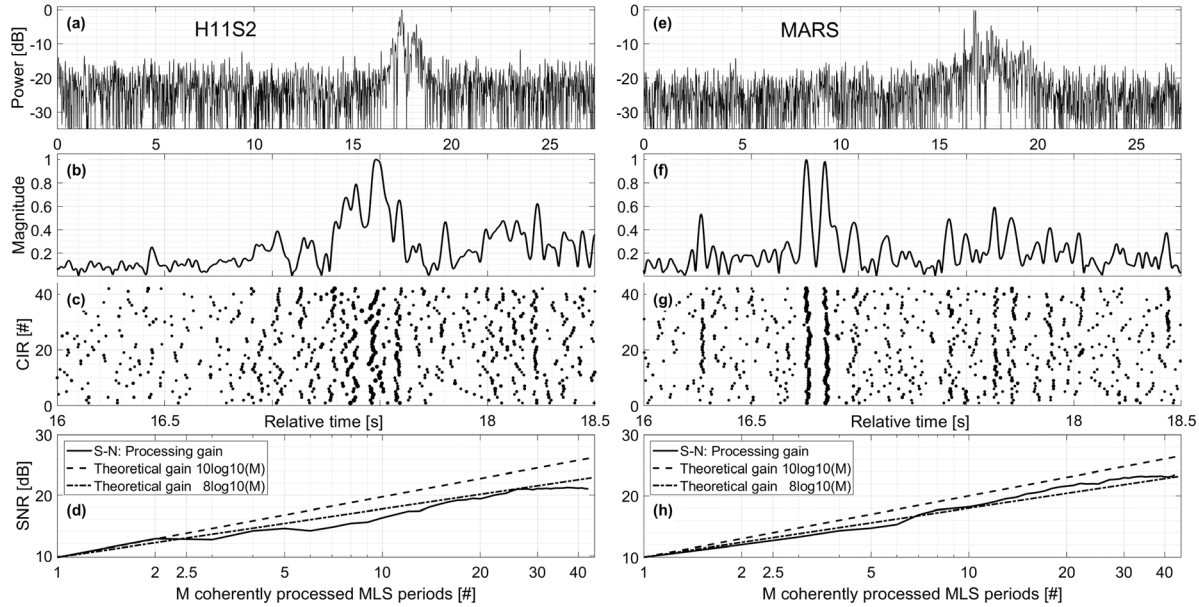


Fig. 2. Processing results for 20 min Tx number 4 (Table 2) received at stations H11S2 [(a)–(d)] and MARS [(e)–(h)]. [(a),(e)] Normalized channel impulse responses (CIRs) estimate is depicted for $M = 43$ averaged m -sequence receptions, [(b),(f)] sub-segments of respective top panels show CIR structure details, [(c),(g)] 30 highest CIR peaks, each averaged over 2 processed periods, sliding from 1–2 to 42–43 periods are shown, and [(d),(h)] PG is compared to theoretical gain for increasing M . The signal power, S , corresponds to the highest peak observed over 15–20 s [see (a) and (e)] and the noise power estimate, N , is the variance of the matched-filter output computed over 0–10 s.

between 15 and 20 s relative time in Figs. 2(a) and 2(e). The noise power is the variance of the matched-filter output computed over 0–10 s. For normalized CIRs, the noise power is less than -20 dB at H11S2 and MARS.

The temporal analyses in Figs. 2(b), 2(c), 2(f), and 2(g) highlight details of 16–18.5 s relative-CIR structure, evolving over the ~ 19.5 min ($M = 43$ periods) processed receptions. Two dominant paths near 17 s in Fig. 2(g) indicate exceptional signal stability over the transmission duration, driving a nominal PG of $8 \log_{10}(M)$ in Fig. 2(h). In comparison, for receiver H11S2 in Fig. 2(c), dominant paths around 17.5 s seem more variable and, thus, PG in Fig. 2(d) is less than (but similar to) that in Fig. 2(h).

Following Ref. 15, Table 3 lists the signal-to-noise ratio (SNR) accounting for Tx number 4 at both receivers. The volumetric spreading loss is uncertain and attenuation is calculated separately. The noise power estimate at 75 Hz center frequency (1 Hz band) is the variance calculated over 37.5–112.5 Hz during a time when the signal is not present. This value is adjusted by a constant for a nominally flat spectrum of width $2/T_d = 75$ Hz (m -sequence mainlobe zero-crossing to zero-crossing) to yield the noise level (NL). In the absence of additional observations, we assume a coherent pulse-compression gain [note that each “dot-plot” row in Figs. 2(c) and 2(g) is an average across two consecutive receptions]. Due to the observed temporal channel variability across 42 realizations [the dot-plot columns in Figs. 2(c) and 2(g) and calculated PG in Figs. 2(d) and 2(h)], the averaging gain is fit to $8 \log_{10}(M)$.

m -sequences are sensitive to Doppler (waveform dilation)⁹ with application to navigating moving receivers and monitoring deep-sea currents. The scenario in Fig. 1(a) allows for analysis of a single transmission for waveform dilation at different receivers. Receiver MARS is rigidly mounted in a tripod about 1 m off the bottom while receiver H11S2 is suspended in the water column and connected to a roughly 450 m long riser cable. Further, the Global Hybrid Coordinate Ocean Model (HYCOM)¹⁶ predicts currents with an amplitude exceeding 10 cm/s near Wake Island.

Theoretical ambiguity surfaces for the m -sequence in Table 1 indicate a nominal ambiguity (-3 dB points) in Doppler of about ± 30 cm/s for a single processed m -sequence period, reducing to less than ± 1 cm/s for 43 averaged periods (not shown). Ambiguity surfaces in Figs. 3(a) and 3(d) extend results in Figs. 2(a) and 2(d) for a waveform dilation analysis over ± 8 cm/s for 43 averaged periods. The observed Doppler spread (radial velocity) for most paths, approximately, is ± 1 cm/s, which is similar to theoretical predictions. Two horizontal, white dashed-dotted lines separated by 3 cm/s and superimposed on the ambiguity surfaces bound most of the spread. The lines are centered at 0 cm/s for MARS in Fig. 3(d) and offset to 0.5 cm/s for H11S2 in Fig. 3(a), thus, indicating a closing range for hydrophone H11S2.

A PG analysis in Fig. 3(b) with two different dilations for the path marked with the white arrow in Fig. 3(a) reveals a gain increase for 1 cm/s over 0 cm/s when averaging more than ten m -sequence periods. The theoretical Doppler ambiguity for ten averages is about ± 3.5 cm/s, which can be prohibitive to distinguish between nearly identical waveform dilations (0

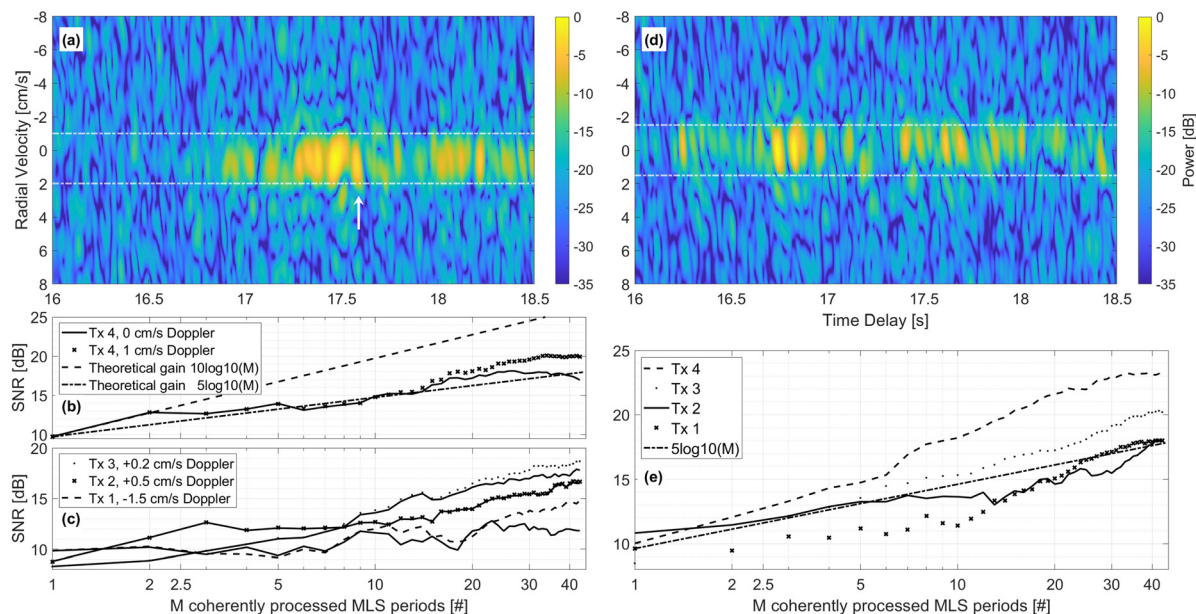


Fig. 3. Tx numbers 1–4 analyses for H11S2 [(a)–(c)] and MARS [(d) and (e)]. Station H11S2 is suspended into the Sound Fixing and Ranging Channel (SOFAR) channel, and the MARS receiver is mounted near the seafloor. Ambiguity surfaces in (a) and (d) extend Figs. 2(b) and 2(f) for Tx number 4 to include waveform dilation, and the white dashed lines are 3 cm/s apart. The PG of the single signal-peak marked with a white arrow in (a) is evaluated at 0 cm/s and +1 cm/s in (b). Similar to (a) and (b), (c) shows Tx numbers 1–3 processing. The PG at selected waveform dilations (see the legend) exceeds or is similar to the non-dilated PG (closest continuous black line). (e) MARS PG (no waveform dilation) for Tx numbers 1–4 is compared to $5 \log_{10}(M)$.

and 1 cm/s). As resolution is proportional to the number of processed and averaged m -sequence periods, sufficient averaging and constant receiver velocity is required to identify and monitor waveform dilation at receiver H11S2 near Wake Island.

Similarly, this analysis is extended to receptions 1–3 in Fig. 3(c). It is noteworthy that Tx number 1 is analyzed at -1.5 cm/s, which is very different from the other transmissions. A waveform dilation of -1.5 cm/s [same y -intercept as the top, white dashed-dotted line in in Fig. 3(a)] would produce an insignificant gain if uncompensated. A constant sampling rate anomaly for receiver H11S2, therefore, can be excluded.

4. Future utility of the nascent source and receiver network

The KB source, along with the nascent receiver network shown in Fig. 1(a), allows for thermometry investigations into the variability of large-scale ocean temperatures. Wake Island hydrophone data can be queried readily from public databases, e.g., through the IRIS (Incorporated Research Institutions for Seismology) data repository¹⁷ to generate near real-time analysis of these transmissions. Also, the IRIS database includes hydrophones of the OOI (Ocean Observatories Initiative) Regional Scaled Nodes (RSN, now called Regional Cabled Array) network, which monitors a seismically active area 400 km off the coast of Oregon. Although not depicted here, we intend to report results from processing data archived by IRIS as well as from additional observatories (such as the Ocean Networks Canada), in a future publication.

Relevant future basin scale applications include investigations into the value-added of the high-resolution Fleet Numerical Meteorology and Oceanography Center (FNMOC) Navy Global HYCOM to predict transmission loss and arrival times over seasonal or annual sound speed field averages. The addition of diverse assimilated tomographic observations, modeled and measured, would reduce the uncertainty of ocean state estimates.^{5,18–21}

Last, time series of travel time will inform us on long-term changes in average ocean temperatures. Ongoing basic research includes investigations into comparing the observed to the modeled multipath arrival structure and scattering effects, as well as the assimilation of the travel time data into ocean models.

Acknowledgments

This research is supported by the Office of Naval Research under Grant No. N00014-23-WX-0-1779 and the Naval Postgraduate School. We acknowledge the Comprehensive Nuclear Test Ban Treaty Organization (CTBTO) for providing Wake Island hydrophone data. The National Science Foundation (NSF) supports the acquisition of the acoustic data at the ALOHA Cabled Observatory under Grant Nos. 1926188 and 2220319.

References

- ¹M. A. McDonald, J. A. Hildebrand, and S. Mesnick, "Worldwide decline in tonal frequencies of blue whale songs," *Endang. Spec. Res.* **9**(1), 13–21 (2009).
- ²M. Gassmann, S. M. Wiggins, and J. A. Hildebrand, "Deep-water measurements of container ship radiated noise signatures and directionality," *J. Acoust. Soc. Am.* **142**(3), 1563–1574 (2017).
- ³T. G. Birdsall and K. Metzger, "Factor inverse matched filtering," *J. Acoust. Soc. Am.* **79**(1), 91–99 (1986).
- ⁴W. Munk, P. Worcester, and C. Wunsch, *Ocean Acoustic Tomography* (Cambridge University Press, Cambridge, UK, 1995), pp. 197 and 206.
- ⁵B. D. Dushaw, "Surprises in physical oceanography: Contributions from ocean acoustic tomography," *Tellus A: Dyn. Meteorol. Oceanogr.* **74**(2022), 33–67 (2022).
- ⁶B. M. Howe, J. Miksis-Olds, E. Rehm, H. Sagen, P. F. Worcester, and G. Haralabus, "Observing the oceans acoustically," *Front. Mar. Sci.* **6**(July), 426 (2019).
- ⁷B. M. Howe, S. G. Anderson, A. Baggeroer, J. A. Colosi, K. R. Hardy, D. Horwitz, F. W. Karig, S. Leach, J. A. Mercer, K. Metzger, L. R. O. Olson, D. A. Peckham, D. A. Reddaway, R. R. Ryan, R. P. Stein, K. von der Heydt, J. D. Watson, S. L. Weslander, and P. F. Worcester, "Instrumentation for the acoustic thermometry of ocean climate (ATOC) prototype Pacific Ocean network," in *Oceans Conference Record* (IEEE, New York, 1995), Vol. 3, pp. 1483–1500.
- ⁸J. C. Steinberg and T. G. Birdsall, "Underwater sound propagation in the Straits of Florida," *J. Acoust. Soc. Am.* **39**(2), 301–315 (1966).
- ⁹K. L. Gemba, H. J. Vazquez, J. Fialkowski, G. F. Edelmann, M. A. Dzieciuch, and W. S. Hodgkiss, "A performance comparison between *m*-sequences and linear frequency-modulated sweeps for the estimation of travel-time with a moving source," *J. Acoust. Soc. Am.* **150**(4), 2613–2623 (2021).
- ¹⁰S. J. Gibbons, "The hydroacoustic network of the CTBT International Monitoring System: Access and exploitation," *J. Peace Nucl. Disarmament* **5**(2), 452–468 (2022).
- ¹¹K. B. Smith, P. Leary, T. Deal, J. Joseph, J. Ryan, C. Miller, C. Dawe, and B. Cray, "Acoustic vector sensor analysis of the Monterey Bay region soundscape and the impact of COVID-19," *J. Acoust. Soc. Am.* **151**(4), 2507–2520 (2022).
- ¹²GEBCO Bathymetric Compilation Group, "The GEBCO 2021 Grid: A continuous terrain model of the global oceans and land," in *NERC EDS British Oceanographic Data Centre NOC* (NERC EDS British Oceanographic Data Centre NOC, Southampton, UK, 2021).
- ¹³M. D. Vera and K. D. Heaney, "The effect of bottom interaction on transmissions from the North Pacific Acoustic Laboratory Kauai source," *J. Acoust. Soc. Am.* **117**(3), 1624–1634 (2005).
- ¹⁴APL, "APL-UW high-frequency ocean environmental acoustics model handbook," APL-UW TR 9407 (Applied Physics Laboratory, University of Washington, Seattle, WA, 1994).
- ¹⁵R. C. Spindel, "An underwater acoustic pulse compression system," *IEEE Trans. Acoust., Speech, Signal Process.* **ASSP-27**(6), 723–728 (1979).
- ¹⁶E. J. Metzger, O. M. Smedstad, P. G. Thoppil, H. E. Hurlburt, J. A. Cummings, A. J. Wallcraft, L. Zamudio, D. S. Franklin, P. G. Posey, M. W. Phelps, P. J. Hogan, F. L. Bub, and C. J. Dehaan, "US Navy Operational Global Ocean and Arctic Ice Prediction Systems," *Oceanography* **27**(3), 32–43 (2014).
- ¹⁷V. Institutions, "International miscellaneous stations" (1965), available at <https://www.fdsn.org/networks/detail/IM/> (Last viewed July 27, 2023).
- ¹⁸M. I. Yaremchuk and A. I. Yaremchuk, "Variational inversion of the ocean acoustic tomography data using quadratic approximation to travel times," *Geophys. Res. Lett.* **28**(9), 1767–1770, <https://doi.org/10.1029/2000GL012287> (2001).
- ¹⁹G. Gopalakrishnan, B. D. Cornuelle, M. R. Mazloff, P. F. Worcester, and M. A. Dzieciuch, "State estimates and forecasts of the Northern Philippine Sea circulation including ocean acoustic travel times," *J. Atmos. Ocean. Technol.* **38**(11), 1913–1933 (2021).
- ²⁰K. L. Gemba, J. Sarkar, B. Cornuelle, W. S. Hodgkiss, and W. A. Kuperman, "Estimating relative channel impulse responses from ships of opportunity in a shallow water environment," *J. Acoust. Soc. Am.* **144**(3), 1231–1244 (2018).
- ²¹K. L. Gemba, H. J. Vazquez, J. Sarkar, J. D. Tippmann, B. D. Cornuelle, W. S. Hodgkiss, and W. A. Kuperman, "Moving source ocean acoustic tomography with uncertainty quantification using controlled source-tow observations," *J. Acoust. Soc. Am.* **151**(2), 861–880 (2022).